

Reaction of Hydroxyl Radical with Aromatic Hydrocarbons in Nonaqueous Solutions: A Laser Flash Photolysis Study in Acetonitrile

James S. Poole,*[†] Xiaofeng Shi, Christopher M. Hadad,* and Matthew S. Platz*

Department of Chemistry, The Ohio State University, 100 West 18th Avenue, Columbus, Ohio 43210

Received: October 20, 2004; In Final Form: January 14, 2005

Laser flash photolysis (LFP) of acetonitrile solutions of *N*-hydroxypyridin-2-thione in the presence of *trans*-stilbene generates a transient absorbance at 392 nm, attributed to the addition of hydroxyl radical to stilbene. The observed transient absorbance was used in competitive LFP experiments to determine relative rates of reaction for hydroxyl radical with a range of aromatic hydrocarbons in acetonitrile. Structure–reactivity relationships for the reaction of hydroxyl radical with arenes are derived. With these aromatic hydrocarbons, we observe a good correlation between the rates of hydroxyl-radical reaction and the ionization potential of the arene. Kinetic isotope effects are consistent with hydroxyl-radical addition being the dominant reaction pathway with the arene.

Introduction

It is now well accepted that a number of reactions of importance to both biological¹ and environmental² chemists require the intermediacy of a group of compounds known collectively as reactive oxygen species (ROS).³ The term ROS covers a range of different species that contain oxygen, but one of the most reactive and important is the hydroxyl radical (HO[•]). Hydroxyl radical intermediacy is critical in a range of important solution-phase reactions from pollutant photochemistry in natural waters² to the chemistry of aging and carcinogenesis.⁴ As such, this species has received a great deal of attention.

One of the most important components in the study of these complex reactions is our ability to measure the rates of fundamental reactions involving these species. Many groups have studied the kinetics of reaction of hydroxyl radical with organic substrates in the aqueous phase, largely by a combination of laser flash photolysis (LFP)⁵ and pulse radiolysis (PR)⁶ techniques. Much of the data has been compiled and is readily available.⁷

An important group of environmental pollutants are polycyclic aromatic hydrocarbons (PAHs).^{8,9} These compounds are common components of crude oils and are also highly publicized products of fossil fuel combustion. One of the characteristics of these compounds is their low solubility in water, making them difficult to study in aqueous solutions on the laboratory scale. However, the high reactivity of hydroxyl radical with most polar organic compounds (including solvents) makes it difficult to perform nonaqueous experiments.

This paper describes the measurement of rate coefficients for reaction of hydroxyl radical with aromatic hydrocarbons by a laser flash photolysis technique in acetonitrile solution. We exploit the relatively slow reaction of hydroxyl radical with acetonitrile⁷ to allow us to probe its reactivity with a variety of aromatic hydrocarbons in this solvent. We use these kinetic data to derive structure–reactivity relationships for hydroxyl radical reactions with a diverse set of aromatic hydrocarbons.

Experimental Details

High-performance liquid chromatography grade acetonitrile, *trans*-stilbene, and *N*-hydroxypyridin-2-thione were obtained from Aldrich and used as received. All other materials (95–99%+ purity) were obtained from Aldrich; crystalline solids were used as received, and liquids were passed through a short column of basic alumina prior to use. Solutions (2 mL) consisting of *N*-hydroxypyridin-2-thione (5×10^{-4} M), *trans*-stilbene (held constant between 0.01 and 0.015 M), and the aromatic competitor (serial concentrations between 0.00 and 1.10 M, depending on the reactivity of the competitor) were deoxygenated using a thin stream of bubbling argon. The concentrations of *N*-hydroxypyridin-2-thione (PSH) and *trans*-stilbene were chosen to provide optimal signal intensity from the system (an overall optical density for PSH of about 1.8–2.0 at 355 nm). Solutions were photolyzed at 355 nm, and the transient absorbance signal was monitored at 392 nm. The instruments for the transient UV–vis spectroscopic and nanosecond laser flash photolysis kinetic measurements have been described previously.¹⁰

Results and Discussion

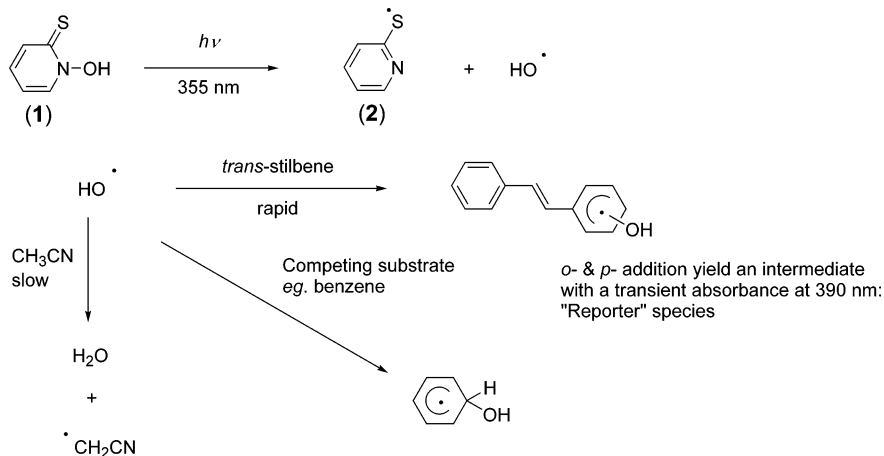
The LFP technique used to determine the rate coefficients for hydroxyl radical reactions has been described in detail in a previous report.¹¹ To summarize, hydroxyl radical is generated by the photolysis of *N*-hydroxypyridin-2-thione (**1**, Scheme 1)¹² in acetonitrile with a 355-nm laser pulse (nominal pulse width = 10 ns).

The formed hydroxyl radical reacts with *trans*-stilbene to generate transient species that absorb around 392 nm. Calculations¹¹ suggest that the intermediates responsible for this signal arise from hydroxyl radical addition to the aromatic ring in the ortho or para position (Scheme 1). The absolute second-order rate constant for the reaction of hydroxyl radical with *trans*-stilbene in acetonitrile has been determined to be $(6.1 \pm 0.2) \times 10^9 \text{ M}^{-1} \text{ s}^{-1}$ by measuring the pseudo-first-order rate constant of formation of transient absorption as a function of *trans*-stilbene concentration.¹¹ This is the sum of all rate constants for all modes of reaction of hydroxyl radical with *trans*-stilbene.

* Authors to whom correspondence may be addressed. E-mail: hadad.1@osu.edu. E-mail: jspoole@osu.edu. E-mail: platz.1@osu.edu.

[†] Current address: Department of Chemistry, Ball State University, Muncie, IN 47306.

SCHEME 1: Chemical Reactions Involved in LFP Methodology



The signal at 392 nm is due to two processes. One is the fast reaction of hydroxyl radical to produce the species discussed above, which are also consumed on the time scale of the LFP experiment. The second process slowly generates species that are persistent on the time scale of the fast reactions mentioned previously. It is likely that the slow process or processes correspond to secondary reactions of pyridyl radical (2), most likely dimerization or reaction with formed cyanomethyl or other radicals.^{11,12} The time scales of these two processes are sufficiently different so that to a good approximation, the two processes may be considered separable for the purposes of Stern–Volmer analysis. That is, the slow growth curve in the absence of *trans*-stilbene may be subtracted from the combined signal to yield a growth and decay curve for the rapidly formed intermediate.

Monitoring the yield of transient absorption at 392 nm enables us to determine the relative rate coefficients for competitive reactions of hydroxyl radical with *trans*-stilbene and a given aromatic substrate by a Stern–Volmer analysis (see Supporting Information) according to the equation below

$$\frac{A_{\text{stilbene-HO}}^{\circ}}{A_{\text{stilbene-HO}}} = 1 + k_{\text{arene}}\tau$$

where $A_{\text{stilbene-HO}}^{\circ}$ is the optical yield of the stilbene–HO adduct in acetonitrile, $A_{\text{stilbene-HO}}$ is the optical yield of the stilbene–HO adduct in the presence of stilbene and arene, k_{arene} is the absolute second-order rate constant for the reaction of arene with HO radical, and τ is the lifetime of the HO radical in the presence of constant stilbene concentration but in the absence of arene. Previously, we have shown that $k_{\text{stilbene}} = (6.1 \pm 0.2) \times 10^9 \text{ M}^{-1} \text{ s}^{-1}$ in acetonitrile at ambient temperature.¹¹ At the concentrations of stilbene of 0.010–0.015 M used in this work, $k_{\text{stilbene}}[\text{stilbene}] \gg k_{\text{T}}$ (where k_{T} represents the sum of all rate constants for all processes which consume hydroxyl radical in the absence of stilbene) and

$$\frac{A_{\text{stilbene-HO}}^{\circ}}{A_{\text{stilbene-HO}}} = 1 + \frac{k_{\text{arene}}[\text{arene}]}{k_{\text{stilbene}}[\text{stilbene}]}$$

The concentration of stilbene is kept constant with a particular arene. It is important to note that k_{arene} and k_{stilbene} are the total of all rate constants for reaction of HO radical with the arene and stilbene, respectively, at all sites and by both addition and hydrogen-atom abstraction mechanisms. Typical Stern–Volmer data obtained from competitive experiments between *trans*-stilbene and toluene and *m*-xylene and *p*-xylene at 298 K are

shown in Figure 1. The relative rate coefficients for reaction of hydroxyl radical with *trans*-stilbene and aromatic substrates determined by Stern–Volmer analysis of kinetic data obtained by this method are summarized in Table 1. The data relate to a number of aromatic substrates, including benzene, benzene-*d*₆, and naphthalene, which have been discussed in our previous report.¹¹ Where data are available, we have included the values obtained by LFP and PR studies in aqueous solutions.⁷

Solvent Effects. As we have noted previously,¹¹ the rate coefficients for reactions of hydroxyl radical with arenes in acetonitrile are significantly smaller than those observed in water, an unexpected result. High-level ab initio and density functional theory calculations performed on the hydroxyl radical/benzene system in both water and acetonitrile indicate that the hydroxyl radical is stabilized by favorable hydrogen-bonding interactions with water, an option not available to this species in acetonitrile. However, the transition state for the hydroxyl radical/benzene system is stabilized to an even greater extent in water than in acetonitrile. Thus, the stabilization of the reactants in water due to solvation is offset by the even greater stabilization of the transition state in water.¹¹

For the data available, the ratio of rate coefficients for HO• reaction with arenes in water relative to acetonitrile (Table 1)

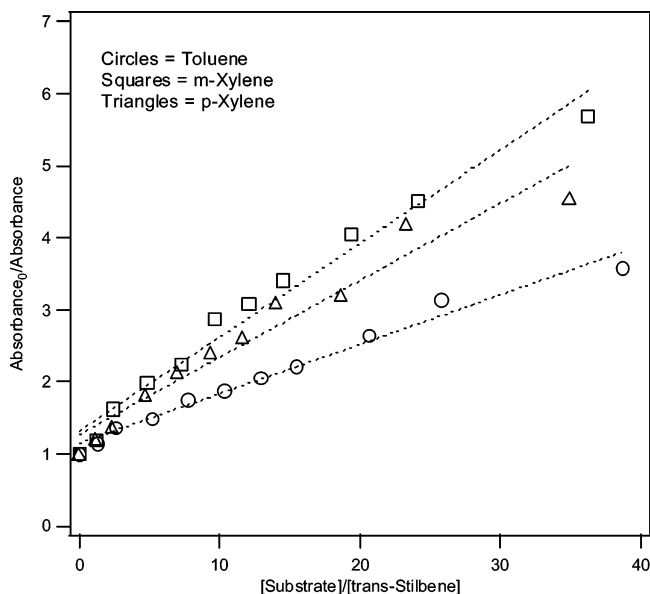


Figure 1. Stern–Volmer data obtained from competitive experiments between *trans*-stilbene and toluene (○), *m*-xylene (□), and *p*-xylene (△) at 298 K. The dotted lines are lines of best fit, and the relative rate coefficients obtained from these experiments are shown in Table 1.

TABLE 1: Summary of Kinetic Data for Reaction of Hydroxyl Radical with Aromatic Hydrocarbons

substrate	$k_{\text{arene}}/k_{\text{stilbene}}^a$	R^2^b	$k_{\text{arene,ACN}}^c$ ($\text{M}^{-1} \text{s}^{-1}$)	$k_{\text{arene,aq}}^d$ ($\text{M}^{-1} \text{s}^{-1}$)	IP ^e (eV)
benzene	0.0209 ± 0.0012	0.98	$(1.2 \pm 0.1) \times 10^8$	$7.8 \times 10^9^f$	9.243
benzene- <i>d</i> ₆	0.0198	0.98	$(1.2 \pm 0.1) \times 10^8$	$4.7 \times 10^9^f$	
toluene	0.0686 ± 0.0034	0.99	$(4.2 \pm 0.2) \times 10^8$	5.1×10^9	8.828
toluene- <i>d</i> ₃	0.0620	0.99	$(3.8 \pm 0.1) \times 10^8$		
toluene- <i>d</i> ₅	0.0571	0.99	$(3.5 \pm 0.1) \times 10^8$		
toluene- <i>d</i> ₈	0.0587	0.99	$(3.6 \pm 0.1) \times 10^8$		
<i>o</i> -xylene	0.107	0.99	$(6.5 \pm 0.2) \times 10^8$	6.7×10^9	8.56
<i>m</i> -xylene	0.130 ± 0.007	0.99	$(7.9 \pm 0.5) \times 10^8$	7.5×10^9	8.55
<i>p</i> -xylene	0.107 ± 0.008	0.97	$(6.6 \pm 0.5) \times 10^8$	7.0×10^9	8.44
mesitylene	0.241 ± 0.008	1.00	$(1.5 \pm 0.1) \times 10^9$	6.4×10^9	8.40
durene	0.232 ± 0.008	1.00	$(1.5 \pm 0.1) \times 10^9$		8.06
naphthalene	0.290 ± 0.007	1.00	$(1.8 \pm 0.1) \times 10^9$	9.4×10^9	8.144
1-methylnaphthalene	0.411 ± 0.022	0.98	$(2.5 \pm 0.2) \times 10^9$		7.96
2-methylnaphthalene	0.462 ± 0.021	0.99	$(2.8 \pm 0.2) \times 10^9$		7.91
1,3-dimethylnaphthalene	0.701 ± 0.027	0.91	$(4.3 \pm 0.2) \times 10^9$		7.86
1,4-dimethylnaphthalene	0.845 ± 0.065	0.97	$(5.2 \pm 0.4) \times 10^9$		7.80
biphenyl	0.111 ± 0.007	0.98	$(6.8 \pm 0.5) \times 10^8$	9.5×10^9	8.16
diphenylmethane	0.128 ± 0.011	0.97	$(7.9 \pm 0.7) \times 10^8$		8.9
bibenzyl	0.111 ± 0.007	0.98	$(6.8 \pm 0.5) \times 10^8$		8.9
<i>trans</i> -stilbene			$(6.1 \pm 0.2) \times 10^9$		7.656

^a Determined by Stern–Volmer analysis (298 K) for the variation of observed transient absorbance with increasing concentration of arene substrate.

^b Goodness-of-fit parameter for the line of best fit for Stern–Volmer data. ^c Rate constants in acetonitrile as determined in this work. ^d See compiled data, refs 7 and 15, for rate constants in water. ^e NIST recommended values, see ref 21. ^f See the text (and ref 14) for discussion of KIE experiments with benzene and benzene-*h*₆ in water.

varies from a factor of 65 for benzene down to a factor of 4 for mesitylene. It is expected that as the measured rate coefficient in acetonitrile approaches the diffusion-controlled limit, this factor will become smaller and approach a limiting value of approximately 0.37. This latter value is calculated from the measured viscosities of these solvents at 293 K (0.37 cP for acetonitrile and 1 cP for water) and assumes no change in the reactants' hydrodynamic radii moving from water to acetonitrile. The qualitative behavior of the rate-coefficient ratios is consistent with such an expectation.

Kinetic Isotope Effects (KIE). The absence of a significant KIE for benzene and benzene-*d*₆¹¹ is consistent with the fact that the dominant reaction of hydroxyl radical with benzene is addition to the ring rather than hydrogen-atom abstraction at the phenyl C–H position.¹³ In fact, the KIE for hydroxyl-radical reaction with benzene in water was measured by Dorfman and co-workers. This is the only reported value using an internally consistent method for both isotopomers.¹⁴ These authors obtained the same rate constant for benzene-*h*₆ and benzene-*d*₆, specifically $4.7 \times 10^9 \text{ M}^{-1} \text{ s}^{-1}$, and therefore no KIE effect was observed in water. (We should note that, since then, there have been multiple measurements of the reaction of hydroxyl radical with benzene, and the consensus rate constant for benzene-*h*₆ in water is slightly faster at $7.8 \times 10^9 \text{ M}^{-1} \text{ s}^{-1}$.^{7,15}) Our acetonitrile rate constants for benzene-*h*₆ and benzene-*d*₆, as well as the aqueous results of Dorfman, concur in that there is no significant KIE for HO• radical reactions with benzene. These results are consistent with a dominant radical-addition reaction with the aromatic ring.

The measured KIE for the toluene isotopomers allows us to determine the importance of hydroxyl radical addition to the aromatic ring relative to hydrogen-atom abstraction from a benzylic position, a more thermodynamically favored process than abstraction from a phenyl C–H position. The hydrogen-atom abstraction reaction would be expected to exhibit a significant primary KIE. However, comparison of the relative rate coefficients of toluene and toluene-*d*₃ yields a KIE of 1.1. Such a result tends to indicate that abstraction at the benzylic position represents a minor reaction pathway, consistent with results obtained previously in the gas phase.¹⁶ It appears that the major influence of the methyl group in the increased

reactivity of toluene relative to benzene (an approximately 3-fold increase) is activation of the aromatic ring. This is confirmed by comparison of toluene with toluene-*d*₅ and toluene-*d*₈. The KIE measured for addition to the ring (toluene-*d*₅) is small, approximately 1.2, as would be expected if H-atom abstraction occurs but is only a minor contributor to the overall reaction rate, and the KIE is little changed by deuteration at the benzylic position (toluene-*d*₈).

We should note as well that a number of rate constants for hydroxyl radical reactions have been measured in the gas phase.⁷ The relative ratio of rate constants between benzene and *p*-xylene is ~12 in the gas phase and only ~5 in acetonitrile between the two substrates. The participation of multiple reaction pathways (addition vs abstraction) and loose complexes on the entrance channel (as the reactants approach each other) may be responsible for this difference.

Structure–Reactivity Relationships. The KIE data for toluene indicate that the relative importance of hydrogen-atom abstraction from the benzylic position is low compared to addition to the aromatic ring. However, as more methyl groups are added to the system under study, we assume that abstraction from a benzylic site should become increasingly probable. Of course, the addition of methyl groups to an aromatic system will also activate the aromatic ring, particularly toward an electrophilic radical such as the hydroxyl radical.¹⁷ We have considered the obtained data from two approaches: one is a purely probabilistic analysis; the other based on a frontier molecular orbital model.

The probabilistic approach is a very simple one: we simply determine the rate coefficient ratio for the system under study relative to its “parent” compound. In the case of benzene and naphthalene derivatives, the “parent” compounds are benzene and naphthalene, respectively; for the remaining compounds in Table 1, biphenyl is chosen as the “parent” compound. The relative rate coefficients are then plotted against the ratio of possible hydrogen-atom abstraction sites and hydroxyl-radical addition sites (i.e., the number of benzylic hydrogen atoms/the number of ring carbon atoms). The obtained plot is shown in Figure 2 and appears to show some degree of correlation. However, such an approach does not explain why mesitylene is as reactive as durene or indeed why methyl- and dimethyl-

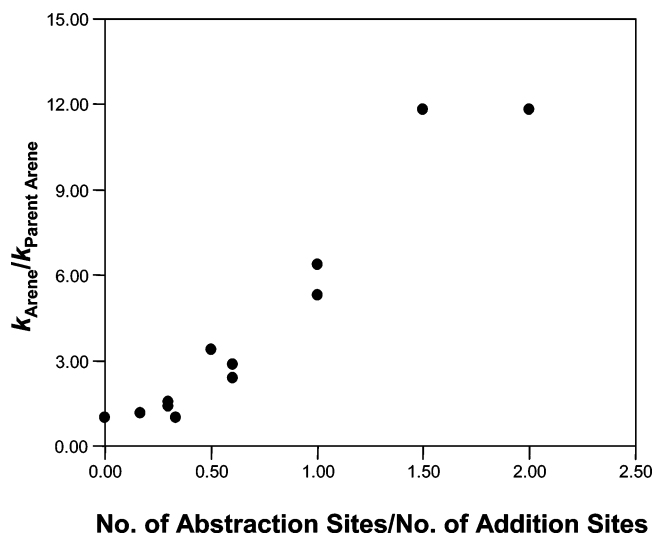


Figure 2. Correlation of the rate coefficient for the reaction of hydroxyl radical with arenes in acetonitrile with a probability-based structure reactivity parameter. The parent arenes used to define the relative rate coefficients are identified in the text.

naphthalene isomers show significantly different reactivity. Moreover, if the probabilistic argument holds true, we would expect that increasing the probability of hydrogen-atom abstraction (presumably the slower of the possible reactions, based on the KIE data from toluene isotopomers) should *decrease* the overall rate of reaction. Therefore, it seems likely that the major influence of the methyl groups is ring activation.

Computational studies of the reaction of hydroxyl radical with benzene indicate that charge-transfer interactions are important in the transition state. In particular, the transition state resembles the hydroxide anion coordinated to the radical cation of benzene.¹¹ This is in excellent agreement with our calculations of the benzene–chlorine atom complex.¹⁸ The frontier molecular orbital model, as developed by Fukui,¹⁹ has been successfully applied to the reactions of alkyl radicals with alkenes by Fischer, Radom, and others.²⁰ This model indicates that the stabilization due to delocalization of an electrophilic radical–arene system as it evolves from reactant to transition state will depend on the energies of the arene highest-occupied molecular orbital and the radical SOMO. Of course, the experimental parameters are the ionization potential (IP) and electron affinity (EA) of the arene and HO radical, respectively. Fischer et al.²⁰ have used a state correlation approach that uses these same parameters to model the energies of the charge-transfer states: the lower the energy of the charge-transfer states, the greater the configurational mixing and stabilization of the ground state. The term “ground state” refers to the lowest electronic energy level of the transition state of reaction. Favorable interactions of the charge-transfer states are those characterized by large values of the parameters ($IP_{\text{arene}} - EA_{\text{HO}^\bullet}$) or ($IP_{\text{HO}^\bullet} - EA_{\text{arene}}$). In this particular case, we will use the first of these parameters as our structure/reactivity parameter.

The IPs for the arenes used in this study have been determined experimentally in the gas phase and are given in Table 1.²¹ Similarly, the electron affinity of hydroxyl radical has been measured in the gas phase and has a value of 1.828 eV.²¹ A plot of $\log(k_{\text{arene}}Ms)$ against ($IP_{\text{arene}} - EA_{\text{HO}^\bullet}$) is shown in Figure 3.

The correlation of the data is quite good, particularly when one considers that the rate coefficients were determined in acetonitrile solution, whereas the structure–reactivity parameter we used was derived solely from gas-phase data. However, it

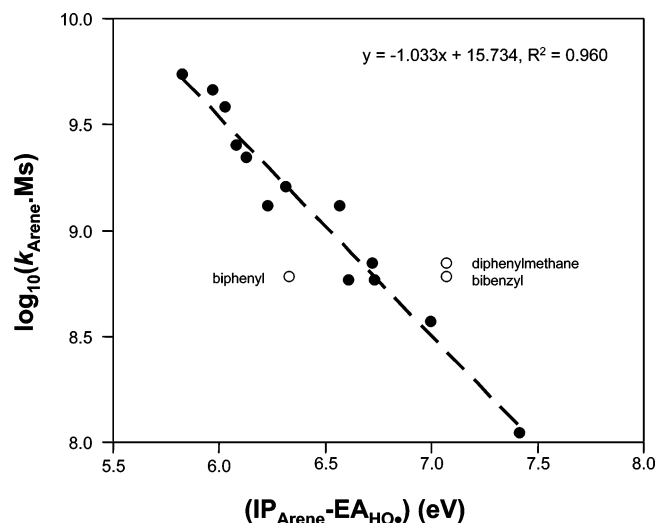


Figure 3. Correlation of the rate coefficient for the reaction of hydroxyl radical with arenes in acetonitrile with the charge-transfer structure/reactivity parameter ($IP_{\text{arene}} - EA_{\text{HO}^\bullet}$). The dashed line and equation correspond to the line of best fit for the data obtained, excluding the data for biphenyl, bibenzyl, and diphenylmethane. If those data are included, the line of best fit is $y = -0.882x + 14.87$, $R^2 = 0.836$.

is worth noting that, for most of these compounds, radical addition to the aromatic ring was the predominant reaction pathway; no other modes of reaction of hydroxyl radical competed with this process to any significant extent. The data obtained for *trans*-stilbene does lie on the correlation curve despite the fact that an attractive, alternative mode of reaction is available to the hydroxyl radical, namely, addition to the alkene double bond. It is difficult to determine whether hydroxyl addition to the alkene carbons competes to any significant extent with the addition to the aromatic ring, but it is worth noting that the phenyl rings may represent a possible steric barrier to reaction at the double bond of *trans*-stilbene. In addition, the transient absorbance observed at 392 nm from reaction of hydroxyl radical with *trans*-stilbene, the basis of our LFP method, appears to be due to the addition of hydroxyl radical to the aromatic ring ortho and/or para to the double bond, based on our earlier calculations.¹¹ It is not clear whether a similarly good correlation would be obtainable for multiply functionalized compounds, and these systems will be studied further in the future.

Conclusions

By use of our LFP-based methodology, we have determined the rate coefficients for the reaction of hydroxyl radical with a number of monocyclic and polycyclic aromatic hydrocarbons in acetonitrile. From an analysis of the observed KIEs for the reaction of hydroxyl radical with isotopomers of benzene and toluene, we conclude that, at least for simple aromatic hydrocarbons, the predominant reaction pathway in acetonitrile is the addition of the hydroxyl radical to the aromatic ring, rather than hydrogen-atom abstraction from the phenyl or, somewhat surprisingly, benzylic C–H positions. Structure–reactivity analysis confirms that addition reactions play a dominant role in more complex systems in acetonitrile: the observed structure–reactivity behavior of these compounds cannot be described in terms of a simple probabilistic model.

A structure–reactivity analysis, based upon frontier molecular orbital and state correlation models, indicates that charge-transfer interactions between a hydroxyl radical and a given arene play an important role in the stabilization of the transition state for

the reaction, an observation in concordance with our earlier computational study of the reaction of hydroxyl radical with benzene.¹¹ A good correlation is observed for the rate coefficient of reaction with the charge-transfer parameter ($IP_{\text{arene}} - EA_{\text{HO}^\bullet}$). It is possible that this relationship may be extrapolated (to a certain extent, the relationship will in all likelihood exhibit limiting behavior at low IP_{arene}) or interpolated to estimate the rate coefficient for reaction of hydroxyl radical with environmentally significant PAHs in solution that cannot be determined by our experimental technique (due largely to spectral interference), provided the gas-phase ionization potential of the hydrocarbon is known. However, we caution against using such a technique for polyfunctionalized compounds; studies of the reactivity of such compounds are currently in progress.

Acknowledgment. Support of this work by the Ohio State University Environmental Molecular Science Institute, funded by the National Science Foundation (CHE-0089147), is gratefully acknowledged.

Supporting Information Available: Further details of Stern–Volmer analysis. This material is available free of charge via the Internet at <http://pubs.acs.org>.

References and Notes

- (1) Zweier, J. L.; Villamena, F. V. Chemistry of Free Radicals in Biological Systems. In *Oxidative Stress and Cardiac Failure*; Kukin, M. L., Fuster, V., Eds.; Futura Publishing Co.: Armonk, NY, 2003; pp 67–95.
- (2) Blough, N. V.; Zepp, R. G. Reactive Oxygen Species in Natural Waters. In *Active Oxygen in Chemistry*; Foote, C. S., Valentine, J. S., Greenberg, A., Liebman, J. F., Eds.; Blackie Academic and Professional: New York, 1995; pp 280–333, Vol. 2.
- (3) (a) Halliwell, B.; Gutteridge, J. M. C. Oxidative stress: adaptation, damage and death. In *Free Radicals in Biology and Medicine*; Oxford University Press: Oxford, 1999; pp 246–350. (b) Roberfroid, M.; Calderon, P. B. *Free Radicals and Oxidation Phenomena in Biological Systems*; Marcel Dekker: New York, 1995.
- (4) (a) von Sonntag, C. *The Chemical Basis of Radiation Biology*; Taylor and Francis, Ltd., London, 1987. (b) Schwarz, H. A. *J. Chem. Educ.* **1981**, *58*, 101–105.
- (5) Scaiano, J. C. Nanosecond laser flash photolysis: a tool for physical organic chemistry. In *Reactive Intermediate Chemistry*; Moss, R. A., Platz, M. S., Jones, M., Jr., Eds.; John Wiley & Sons, Inc.: Hoboken, NJ, 2004; pp 797–845.
- (6) Baxendale, J. H.; Rodgers, M. A. *J. Chem. Soc. Rev.* **1978**, *7*, 235–163. (b) Adams, G. E.; Wardman, P. *Free Radicals Biol.* **1977**, *3*, 53–95.
- (7) A large amount of experimental data has been compiled by the University of Notre Dame Radiation Laboratory supported by the U.S. Department of Energy and in conjunction with the National Institute of Science and Technology: <http://www.rcdc.nd.edu/compilations/Hydroxyl/OH.htm>. Also, the NIST databases are also available online for the gas phase (<http://kinetics.nist.gov>) and for the condensed phase (<http://kinetics.nist.gov/solution>). The absolute rate constant of reaction of HO radical with acetonitrile, in acetonitrile as a solvent, is considerably smaller than the corresponding value in water (see ref 11).
- (8) (a) Schuetzle, D.; Siegl, W. O.; Jensen, T. E.; Dearth, M. A.; Kaiser, E. W.; Gorse, R.; Kreucher, W.; Kulik, E. *Environ. Health Persp.* **1994**, *102* (S4), 3–12. (b) Richter, H.; Howard, J. B. *Prog. Energy Combust. Sci.* **2000**, *26*, 565–608. (c) Marsh, N. D.; Ledesma, E. B.; Sandrowitz, A. K.; Wornat, M. J. *Energy Fuels* **2004**, *18*, 209–217.
- (9) (a) Salloum, M.; Chefetz, B.; Hatcher, P. G. *Environ. Sci. Technol.* **2002**, *36*, 1953. (b) Chefetz, B.; Deshmukh, A. P.; Hatcher, P. G.; Guthrie, E. A. *Environ. Sci. Technol.* **2000**, *34*, 2925.
- (10) Martin, C. B.; Shi, X.; Tsao, M.-L.; Karweik, D.; Brooke, J.; Hadad, C. M.; Platz, M. S. *J. Phys. Chem. B* **2002**, *106*, 10263.
- (11) DeMatteo, M. P.; Poole, J. S.; Shi, X.; Sachdeva, R.; Hatcher, P. G.; Hadad, C. M.; Platz, M. S. *J. Am. Chem. Soc.*, submitted.
- (12) (a) Aveline, B. M.; Kochevar, I. E.; Redmond, R. W. *J. Am. Chem. Soc.* **1996**, *118*, 10124. (b) Aveline, B. M.; Kochevar, I. E.; Redmond, R. W. *J. Am. Chem. Soc.* **1996**, *118*, 10113.
- (13) Barckholtz, C.; Barckholtz, T. A.; Hadad, C. M. *J. Phys. Chem. A* **2001**, *105*, 140–152.
- (14) (a) Dorfman, L.; Taub, I. A.; Buehler, R. E. *J. Chem. Phys.* **1962**, *36*, 3051. (b) Dorfman, L.; Buehler, R. E.; Taub, I. A. *J. Chem. Phys.* **1962**, *36*, 549.
- (15) Buxton, G. V.; Greenstock, C. L.; Helman, W. P.; Ross, A. B. *J. Phys. Chem. Ref. Data* **1988**, *17*, 513–886.
- (16) Atkinson, R. *Atmos. Environ., Part A* **1990**, *24A*, 1–41.
- (17) (a) Minisci, F.; Galli, R. *Tetrahedron Lett.* **1962**, 533–538. (b) Norman, R. O. C.; Radda, G. K. *Proc. Chem. Soc.* **1962**, 138. (c) Cadet, J.; Douki, T.; Gasparutto, D.; Ravanat, J.-L. *Mutation Res.* **2003**, *531*, 5–23.
- (18) Tsao, M.-L.; Hadad, C. M.; Platz, M. S. *J. Am. Chem. Soc.* **2003**, *125*, 8390–8399.
- (19) Fukui, K. *Fortschr. Chem. Forsch.* **1970**, *15*, 1.
- (20) Fischer, H.; Radom, L. *Angew. Chem. Int. Ed.* **2001**, *40*, 1340 and references therein.
- (21) A large amount of data has been compiled by the National Institute of Science and Technology and is available via a searchable database. The website address is <http://webbook.nist.gov/chemistry/>.